

# Interphotoreceptor matrix-poly( $\epsilon$ -caprolactone) composite scaffolds for human photoreceptor differentiation

Petr Baranov<sup>1</sup>, Andrew Michaelson<sup>2</sup>, Joydip Kundu<sup>2</sup>, Rebecca L Carrier<sup>2</sup> and Michael Young<sup>1</sup>

## Abstract

Tissue engineering has been widely applied in different areas of regenerative medicine, including retinal regeneration. Typically, artificial biopolymers require additional surface modification (e.g. with arginine–glycine–aspartate-containing peptides or adsorption of protein, such as fibronectin), before cell seeding. Here, we describe an alternative approach for scaffold design: the manufacture of hybrid interphotoreceptor matrix-poly ( $\epsilon$ -caprolactone) scaffolds, in which the insoluble extracellular matrix of the retina is incorporated into a biodegradable polymer well suited for transplantation. The incorporation of interphotoreceptor matrix did not change the topography of polycaprolactone film, although it led to a slight increase in hydrophilic properties (water contact angle measurements). This hybrid scaffold provided sufficient stimuli for human retinal progenitor cell adhesion and inhibited proliferation, leading to differentiation toward photoreceptor cells (expression of Crx, Nrl, rhodopsin, ROM1). This scaffold may be used for transplantation of retinal progenitor cells and their progeny to treat retinal degenerative disorders.

## Keywords

Retina, photoreceptors, interphotoreceptor matrix, polycaprolactone

Received: 7 August 2014; accepted: 9 September 2014

## Introduction

Transplantation of stem cells or their progeny can be used to treat a large variety of degenerative disorders affecting organs with limited regenerative capacity, such as the nervous system and sensory organs including the eye.<sup>1</sup> Although experimental studies have shown the potential of progenitor cells delivered as single-cell suspensions to integrate into degenerating retina,<sup>2–4</sup> a tissue engineering approach incorporating biomaterials together with cells is particularly promising due to increased cell survival and directed cell differentiation.<sup>5</sup> This is based on a variety of studies involving both natural biopolymers, such as gelatin,<sup>6</sup> chitosan,<sup>7</sup> alginate,<sup>8</sup> and artificial polymers, including poly(lactic-co-glycolic acid) (PLGA),<sup>9</sup> poly(methyl methacrylate) (PMMA),<sup>10</sup> poly(glycerolsebacate) (PGS),<sup>11</sup> poly(hydroxybutyrate) (PHB),<sup>12</sup> and poly( $\epsilon$ -caprolactone) (PCL).<sup>13</sup> These polymers provide a structural scaffold for cell growth and are intended to mimic the natural tissue niche.

The extracellular matrix structure and topography (e.g. basement membranes, fibrillar matrix) are often considered during the design of tissue engineering scaffolds. Porous scaffolds, which allow cell ingrowth, are representative of matrices encountered in connective/muscular/nerve tissue regeneration, while epithelial cells (including neuroepithelial) grow on a relatively flat basement membrane. PLGA and PCL films are suitable scaffolds for mouse and human

<sup>1</sup>The Schepens Eye Research Institute, Massachusetts Eye and Ear, Harvard Medical School, Boston, MA, USA

<sup>2</sup>Department of Chemical Engineering, Northeastern University, Boston, MA, USA

### Corresponding author:

Petr Baranov, The Schepens Eye Research Institute, Massachusetts Eye and Ear, Harvard Medical School, 20 Staniford Street, Boston, MA 02114, USA.

Email: petr.baranov@schepens.harvard.edu



retinal progenitor cells (hRPCs),<sup>14</sup> resulting in robust cell integration into degenerating retina upon implantation and controlled differentiation. The precise mechanisms of material-driven fate specification are yet to be elucidated, although it is suggested that this phenomenon is mediated by surface physical (such as stiffness) or chemical properties, since PCL induces photoreceptor differentiation from hRPCs independently of microtopography. This is confirmed by work with neuron differentiation on electrospun PCL.<sup>15,16</sup> Despite impressive ability of PCL to induce differentiation in these studies, its hydrophobic nature requires additional modification or coating of the surface with charged molecules, such as poly-D-lysine and/or extracellular matrix proteins, including fibronectin, laminin, or collagen to enable efficient cell attachment.<sup>17</sup> An alternative is the incorporation of the extracellular matrix proteins<sup>18</sup> or total extracellular matrix (ECM) fraction<sup>19</sup> into the polymer. Optimally, the incorporated molecules should provide both adhesive properties and differentiation stimuli<sup>12</sup> to the attached cells. This can be achieved with single proteins (fibronectin, laminin) or with tissue-specific decellularized ECM preparations. In the retina, the interphotoreceptor matrix (IPM) is the specialized matrix surrounding the outer segments of photoreceptors.<sup>20</sup> IPM mediates key interactions between the photoreceptors and retinal pigment epithelium (RPE) including adhesion, outer segment stability, nutrient exchange, and trafficking of retinol isoforms in the visual cycle.<sup>21,22</sup> Thus, IPM is a logical matrix to explore for incorporation into hRPC culture or cell delivery biomaterials.

The aim of this study is to elucidate the impact of incorporation of IPM on the differentiation process of hRPCs on PCL films. We have incorporated IPM into PCL and have shown that this composite scaffold, without additional modification, has improved adhesive properties and can drive photoreceptor differentiation of hRPCs.

## Materials and methods

### *IPM isolation and characterization*

The IPM was isolated from adult bovine eyes collected fresh from the abattoir (Research 87 Inc., Boston, MA, USA) within 2 h after slaughter. Briefly, the muscle was removed from the outside of the eye. An incision was made 0.5 cm behind limbus, and a complete circumferential cut was made, being careful not to cut through the vitreous humor. Next, the cornea and vitreous humor were removed from the eye. Phosphate-buffered saline (PBS) was then immediately poured into the eyecup until full. Using a microspatula (Hayman Style), the retina was gently pulled away from the pigmented epithelium. A cut was made through the optic nerve and the retina. The retina was collected using a cut transfer pipette and placed in PBS (Sigma-Aldrich, St. Louis, MO, USA) and then transferred to a Petri dish containing deionized water.

After orbital shaking (3 min, 75 r/min, TECHNE Mini Orbital Shaker, TSSM1, Techne Inc., Burlington, NJ, USA), the retinal debris was removed and the native IPM was collected. The collected IPM was centrifuged (5000 r/min; Sorvall Legen X1R Centrifuge, Thermo Scientific, Waltham, MA, USA) at 25°C for 20 min to pellet the IPM. The PBS was then decanted and the pellet was re-suspended within PBS.

### *PCL and PCL-IPM production*

A total of 10% (w/v) solution of PCL was prepared by dissolving 10 g of PCL (molecular weight (mw) 70,000–90,000; Sigma-Aldrich) in dichloromethane (Sigma-Aldrich) with mixing at room temperature for 24 h. IPM, isolated from 12 bovine eyes, was pelleted (pellet volume approximately 500  $\mu$ L) by centrifuging at 3000g, dehydrated with isopropanol (Sigma-Aldrich), centrifuged, re-suspended in 5 mL of dichloromethane, and then mixed in 100 mL of 10% PCL solution. This preparation was used to prepare two types of scaffolds: films and PCL-IPM-coated plates. The films were prepared as previously described: sufficient volume (5 mL) was poured in the center of a silicone wafer with spinning (Brewer Bioscience, Brewer Science Inc, Rolla, MO, USA) at 2000 r/min for 2 min. The films were dried at 45°C for 30 min, then sterilized by soaking in 95% ethanol for 30 min, and washed in distilled water three times. PCL-coated Petri dishes or coverslips were prepared in the same manner: 60-mm-diameter polystyrene dishes (BD Biosciences, Franklin Lakes, NJ, USA) were fixed on the spinner rotor; 5 mL of PCL (or PCL-IPM) solution was poured in the center; and dishes were spun at 2000 r/min for 5 min. Drying and washing procedures were the same.

### *Characterization of scaffolds: scanning electron microscopy, contact angle, lectin staining*

**Scanning electron microscopy (SEM).** The surface morphology of PCL and PCL-IPM surfaces was observed using an S-4800 Hitachi scanning electron microscope (Los Angeles, CA, USA) at an operating voltage of 3.0 kV. The samples were then attached to a specimen stub with a carbon adhesive tab, sputter coated with 15-nm gold-palladium, and examined at room temperature.

**Contact angle.** Contact angles were measured with static drops of water on PCL and PCL-IPM-coated glass coverslips using a contact angle measurement system (Phoenix 300 plus, SEO, Suwon City, Korea) to provide information about hydrophobicity and hydrophilicity of these surfaces. Each data point represents 10 independent measurements. The experiment was repeated twice.

**Lectin staining.** The lectin staining was performed on PCL and PCL-IPM-coated glass coverslips. The coverslips were

treated with 0.1% bovine serum albumin (Sigma, St. Louis, MO, USA) to prevent non-specific staining. A total of 50  $\mu$ L of FPNA Fluorescein-Labeled Peanut Agglutinin (FPNA; Vector Laboratories) and 50  $\mu$ L (Rhodamine-labeled Wheat Germ Agglutinin (RWGA; Vector Laboratories, Burlingame, CA, USA) were then added to each surface for 30 min in the dark. The staining solutions were then removed, and the surfaces were each flooded with 1 mL of PBS. The surfaces were then examined under a fluorescence microscope.

### *hRPC isolation, expansion, and characterization*

All work with human material was performed with institutional review board (IRB) approval. hRPCs were isolated from human fetal neural retina at 16 weeks of gestational age, as previously described.<sup>23</sup> Briefly, whole neuroretina was peeled from the RPE layer, minced, and digested with collagenase I (Sigma–Aldrich). Cells and clusters were plated onto human fibronectin (Akron, Boca Raton, FL, USA)-coated flasks (Nunclon Delta, Waltham, MA, USA) in Ultraculture Media (Lonza, Walkersville, MD, USA), supplemented with 2 mM L-glutamine (Invitrogen, Carlsbad, CA, USA), 10 ng/mL recombinant human basic fibroblast growth factor (rh-bFGF) (Peprotech, Rocky Hill, NJ, USA), and 20 ng/mL recombinant human epidermal growth factor (rh-EGF) (Peprotech) in low-oxygen incubator (37°C, 3% O<sub>2</sub>, 5% CO<sub>2</sub>, 100% humidity). Fibronectin coating was accomplished by incubating the flasks with 10  $\mu$ g/mL fibronectin solution for 1 h at room temperature (1 mL of the solution per 10 cm<sup>2</sup> of the surface), followed by single wash with deionized water. hRPCs were passaged at 80% confluency using TrypZean (Sigma–Aldrich), benzonase (EMD Chemicals, Darmstadt, Germany), and Defined Trypsin Inhibitor (Invitrogen). At each passage, cell number and viability were estimated with Trypan blue (Sigma–Aldrich) in a hemocytometer, and cells were plated on a fibronectin-coated surface at a density of 20,000 cells/cm<sup>2</sup> in medium. All further described work was performed with a single hRPC cell line at passage 9.

### *hRPC adhesion and proliferation on PCL–IPM scaffolds*

hRPCs were plated at a density of 20,000 cells/cm<sup>2</sup> in 60-mm Petri dishes containing the following materials: IPM–PCL scaffold, uncoated or fibronectin-coated PCL, tissue culture-treated plastic, IPM-coated plastic, or fibronectin-coated plastic, in 3 mL of medium. Fibronectin coating was accomplished as described above; for IPM coating, we incubated the flasks with the IPM suspension for 1 h. The dishes were then incubated for 30 min (37°C, 3% O<sub>2</sub>, 5% CO<sub>2</sub>, 100% humidity) to allow sufficient time for adhesion.<sup>24</sup> After 30 min, all non-attached hRPC were collected, and each well was washed with 3 mL of Hank's Balanced Salt Solution (HBSS) (with Ca<sup>++</sup> and Mg<sup>++</sup>). Collected medium and washes from three wells per group were combined in the

same tube and centrifuged at 400g for 5 min. The numbers of hRPC were counted with a hemocytometer, and the ratio of adhered cells was calculated. This experiment was performed three times (for independent IPM, PCL, and PCL–IPM preparations), and every time three independent Petri dishes were used for each condition. Mean and standard deviation (SD) were calculated for each group for the pooled data, and t-test analysis was performed to compare means.

Since we have previously observed a significant decrease in hRPC proliferation on PCL substrates, we were interested to see whether IPM incorporation leads to any change in this effect. To determine this, hRPCs were plated at a density of 20,000 cells/cm<sup>2</sup> on PCL–IPM, PCL coated with fibronectin, or tissue culture plastic coated with fibronectin in the medium described above, with the medium changed every other day. At days 3 and 7, hRPC cell number was counted by harvesting all the cells as described above for passaging procedure (TrypZean–benzonase). The population doubling (proliferation rate) was calculated based on three separate cell plating experiments. Mean and SD were calculated for each group and the results were compared by t-test.

### *SEM*

To study the effect of incorporation of IPM on the hRPC morphology, we plated cells on fibronectin-coated PCL and PCL–IPM coated-coverslips in the medium described above. After 1 and 7 days, coverslips were washed, fixed, and dehydrated. The coverslips were fixed using 4% paraformaldehyde solution and dehydrated using sequential treatment with 35%, 50%, 70%, 95%, and 100% ethanol. After dehydrating with 100% ethanol, the samples were treated with hexamethyldisilazane (HMDS) and allowed to air dry after being attached to a specimen stub. Dried samples were sputter coated with 15-nm gold–palladium, and the hRPC morphology on PCL and PCL–IPM surfaces was observed using a scanning electron microscope (S-4800 Hitachi) at an operating voltage of 3.0 kV.

### *Photoreceptor differentiation from hRPC on PCL–IPM scaffolds*

To investigate cell differentiation on PCL–IPM scaffolds, we plated hRPC in the medium described above at a density of 20,000 cells/cm<sup>2</sup> on PCL–IPM scaffolds or PCL coated with fibronectin. The medium was replaced every other day. Seven days after plating, live cells were harvested with TrypZean for flow cytometry. hRPCs were fixed in Perm/Fix buffer (BD Biosciences) for 20 min at 4°C. Cells were then washed in Wash buffer (BD Biosciences) and incubated in block buffer (Pharmingen staining buffer with 2% goat serum) for 30 min at room temperature. The cells were stained with primary antibodies for 1 h at room temperature, washed, and stained with secondary conjugated antibodies for 30 min at room temperature. After the final wash, light

scatter and fluorescence signal from each cell were measured by Beckman Epics XL flow analyzer, Beckman Coulter, Brea, CA, USA (10,000 events were recorded). The results were analyzed with FlowJo software (Tree Star, Ashland, OR, USA). The ratio of positive cells within the gated population was estimated based on comparison with species-specific isotype control. For immunocytochemistry, hRPCs were collected after differentiation and replated onto 16-well chamber glass slides, coated with fibronectin. Antibodies used were as follows: anti-Pax6 (1:50; Hybridoma Bank, Iowa City, IA, USA), anti-Lhx2 (1:200; Chemicon, Billerica, MA, USA), anti-Nrl (1:50; Santa Cruz), anti-Crx (1:50; Santa Cruz, Santa Cruz, CA, USA), anti-Recoverin (1:1000; Chemicon), anti-Rhodopsin (1:200; Chemicon), and Anti-Rod Outer Membrane 1 (1:100; Abnova, Walnut, CA, USA).

## Results

### *PCL and PCL–IPM production and characterization of scaffolds*

IPM was successfully isolated from bovine eyes. IPM collection was straightforward as it dissociates from the retina when placed in deionised (DI) water,<sup>20</sup> and numerous macroscopic sheets can be observed and collected. The IPM was successfully incorporated into the polycaprolactone (no chunks of the matrix were observed after mixing with PCL) to produce two types of scaffolds (Figure 1(a)): coated Petri dishes, which eliminate the need to fix the PCL film inside the culture vessel for culture and analysis, and thin films, which can be further used as cell carriers for transplantation purposes.

As was demonstrated by staining with PNA, IPM honeycomb structure observed in collected material (Figure 1(e) and (h)) is lost during PCL–IPM preparation (Figure 1(f)). SEM (Figure 1(b) and (d)) revealed pits in both PCL and PCL–IPM, varying in size from 1 to 7  $\mu\text{m}$ . These pits likely appear during evaporation of the solvent (dichloromethane) from the scaffold. There were no identifiable differences between the topography of PCL and PCL–IPM scaffolds.

### *hRPC adhesion and proliferation on PCL–IPM scaffolds*

IPM incorporation slightly changed the hydrophobic properties of the scaffold, as reflected by mean contact angles of 64.5 in PCL versus 60.2 in PCL–IPM (Figure 2(b)). Although this moderate change was significant, it is unlikely to be the only mechanism causing a profound increase in hRPC adhesion (Figure 2(a)) to the hybrid scaffolds. Coating of plastic with IPM by centrifugation led to a slight increase in adhesion, but we were not able to maintain IPM attachment to the PCL during culture. The inhibitory effect of polycaprolactone on hRPC proliferation did not change (Figure 2(c)) after IPM incorporation: population number

did not increase on polycaprolactone scaffold with IPM to a greater extent than on PCL alone. Due to high proliferation rate, it is not possible to get non-confluent monolayer of hRPC on fibronectin-coated plastic—cells reach overconfluent state, start to form clumps, and detach, resulting in inconsistent cell count.

## SEM

SEM analysis (Figure 3) showed that hRPCs attach and grow processes on the surface of PCL (Figure 3(a) and (b)) and hybrid PCL–IPM (Figure 3(c) and (d)) films. We have observed long cellular processes on all preparations. One-week culture led to stratification (increased area) of cells (Figure 3(b) and (d)), which may be related to additional ECM production and deposition.

### *Photoreceptor differentiation from hRPC on PCL–IPM scaffolds*

One-week culture of hRPC on the PCL scaffolds (both fibronectin-coated and enriched with IPM) led to a significant decrease in the expression of early progenitor markers, such as Pax6 and Lhx2 (Figure 4(a)), while photoreceptor markers (Crx, Nrl, Rhodopsin, Rom1, Recoverin) were upregulated. The immunocytochemical analysis (Figure 4(b)) confirmed the differentiation of hRPC into rod photoreceptors. We did not identify any differences in differentiation pattern between PCL–IPM and PCL coated with fibronectin groups, which suggests that IPM provides stimuli sufficient for photoreceptor differentiation.

## Discussion

Recent advances in retinal regeneration have focused on retinal progenitor and photoreceptor precursor cell transplantation. Several approaches have been investigated,<sup>25</sup> including suspension<sup>26</sup> and composite graft<sup>13</sup> transplantation. Despite a complicated delivery procedure, composite graft transplantation is a promising strategy due to the structural organization and differentiation of cells. The scaffold of choice for such grafts should have properties similar to the ECM of the target tissue. This can be achieved with synthetic or biological polymers with biomimetic structures or chemical composition. One method of scaffold development which has demonstrated great potential is use of decellularized ECM<sup>27</sup> for reconstruction of organs, including vessels,<sup>28</sup> trachea,<sup>29</sup> heart,<sup>30</sup> lungs,<sup>31</sup> and liver.<sup>32,33</sup> These scaffolds not only provide support for the cellular component but also drive differentiation of progenitors and serve as a meshwork for new ECM deposition.

In previous studies with IPM,<sup>21,34</sup> some benefits and limitations have been noted. IPM is the matrix surrounding the outer segments of photoreceptors and is naturally acellular upon collection as described above (as noted by



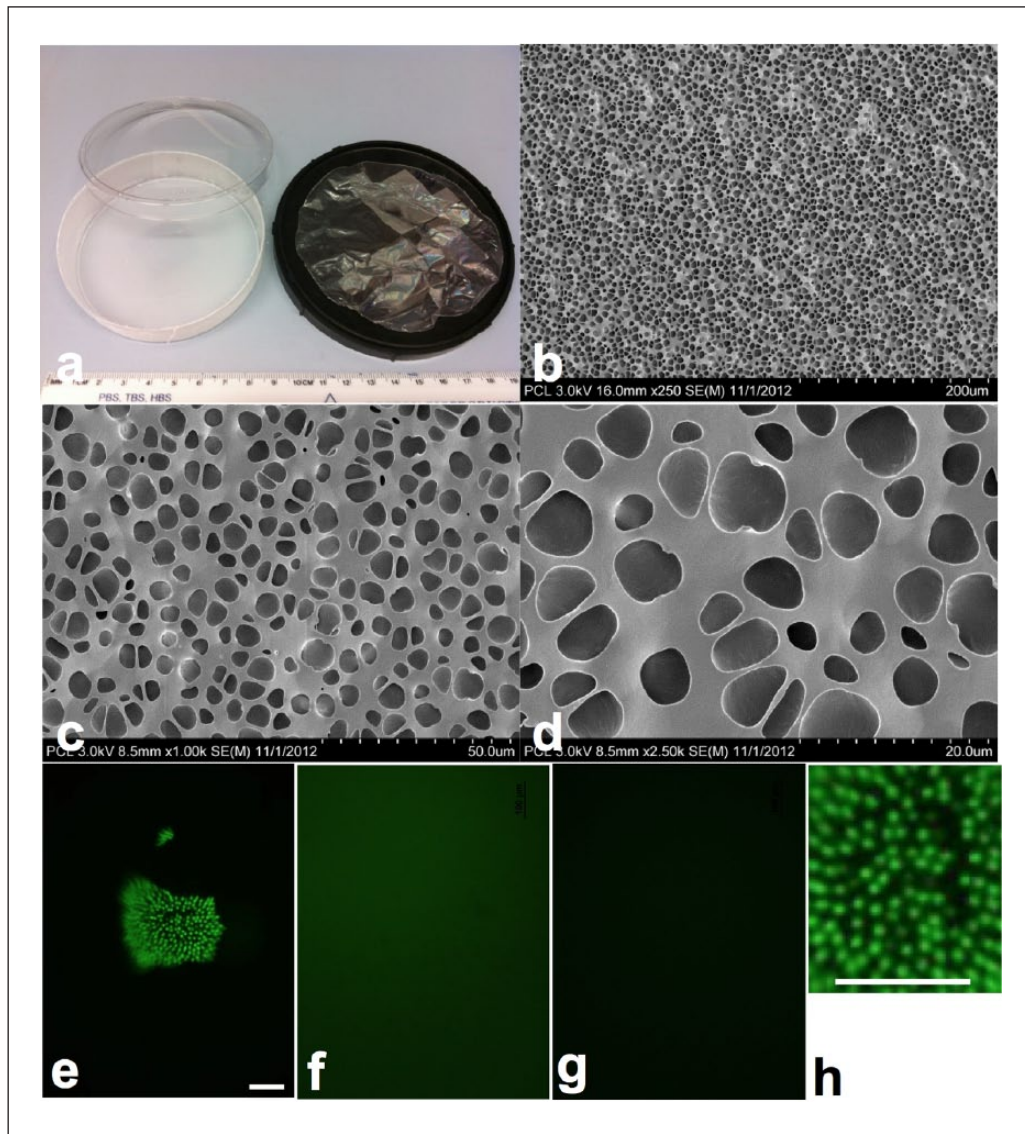


**Figure 1.** PCL and PCL-IPM plates and films. The manufacture of polycaprolactone in 10-cm Petri dish format (a, left) allows the scale up of the cell differentiation, eliminating the need of fixing the thin film (a, right) on the plate. SEM analysis (b–d) on different magnifications has not revealed any differences in the structure of the PCL and PCL-IPM scaffolds. Honeycomb structure of lectins revealed by PNA staining (green) in freshly isolated IPM (e, h) was not preserved during PCL-IPM scaffold preparation, resulting in diffuse staining (f). PCL without any additives (g) was used for control. Bars are 100  $\mu\text{m}$ .

PCL: poly( $\epsilon$ -caprolactone); IPM: interphotoreceptor matrix; SEM: scanning electron microscopy, PNA: peanut agglutinin.

nuclear staining, data not shown). However, in contrast to decellularized bone,<sup>35</sup> blood vessels,<sup>28</sup> trachea,<sup>29</sup> heart,<sup>30</sup> tooth bud,<sup>36</sup> or lacrimal gland, IPM does not possess sufficient mechanical integrity to be easily handled, although we were able to collect it as a suspension. It is possible to use these suspended IPM particles to coat different surfaces by centrifugation, although they tend to detach from the surface, limiting experimental studies. These water-insoluble IPM particles can be suspended in organic solvents, such as dichloromethane or chloroform (trichloromethane), also used for PCL preparation.

This has allowed us to functionalize scaffolds previously described for retinal tissue engineering. Based on our experience with retinal progenitor cells and different types of synthetic polymers<sup>14</sup> (PLGA/poly-L-lactic acid (PLLA),<sup>9</sup> PMMA,<sup>10</sup> PGS,<sup>37</sup> and PCL<sup>38</sup>), we have focused in these studies on PCL due to its biocompatible, biodegradable, and physical properties. We have previously shown that microtopography properties of PCL have only a slight effect on hRPC differentiation.<sup>39</sup>

Although we were able to incorporate IPM, as shown by positive staining for lectin,<sup>40</sup> the honeycomb structure of IPM was lost during this process. The preservation of

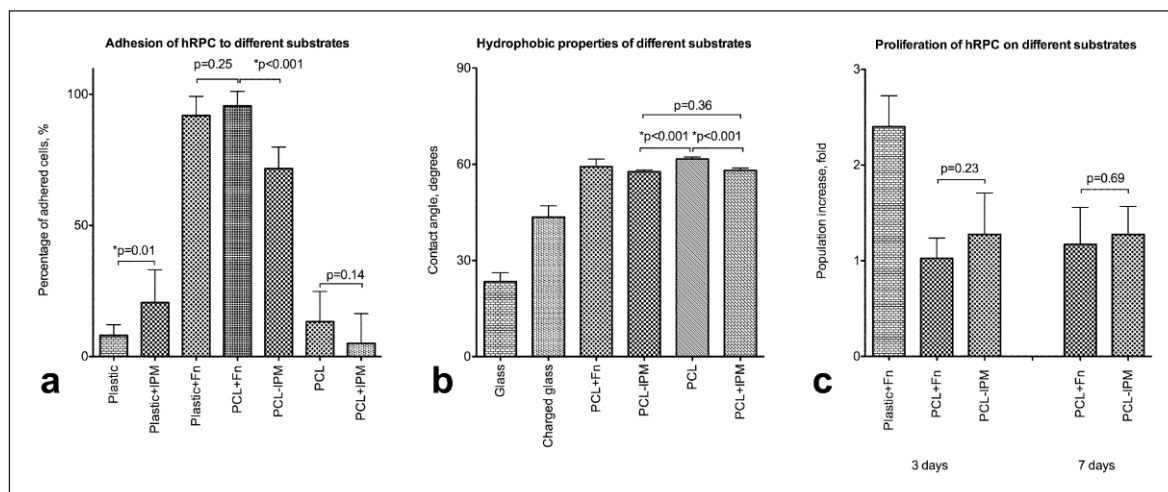


**Figure 2.** Adhesion and proliferation of hRPC on PCL and PCL-IPM. PCL-IPM is slightly more hydrophilic than PCL, based on contact angle measurements (a), which may contribute to the increase in adhesive properties (b). IPM incorporation (PCL-IPM), but not coating (PCL+IPM and plastic+IPM), resulted in significant increase of cells adhered to the substrate after 30 min of incubation. IPM incorporation did not affect the inhibitory effect of PCL on proliferation: cell population has not increased in size after 3 or 7 days of culture (c).

hRPC: human retinal progenitor cell; PCL: poly( $\epsilon$ -caprolactone); IPM: interphotoreceptor matrix.

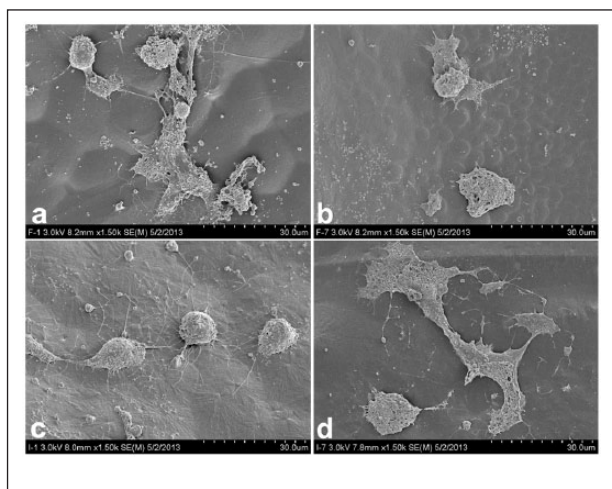


**Figure 3.** hRPC morphology on PCL and PCL-IPM scaffolds. (a) SEM of hRPC on PCL coated with fibronectin day 1, (b) SEM of hRPC on PCL coated with fibronectin day 7, (c) SEM of hRPC on PCL-IPM day 1, and (d) SEM of hRPC on PCL-IPM day 7. hRPC: human retinal progenitor cell; PCL: poly( $\epsilon$ -caprolactone); IPM: interphotoreceptor matrix; SEM: scanning electron microscopy.

this structure is one of the aims for future studies, since it is suggested to be critical for outer segment homeostasis and photoreceptor-RPE interaction.<sup>21</sup> IPM incorporation into PCL leads to a decreased contact angle and increased hRPC adhesion. Although the adhesion is lower compared to fibronectin-coated surfaces, it is sufficient to achieve retinal progenitor cell survival and differentiation. PCL-IPM inhibits proliferation of hRPC in the same manner as

PCL. This inhibition of proliferation is required for differentiation and maturation of photoreceptors. After 1 week on PCL-IPM, retinal progenitor cells obtained photoreceptor phenotype and functional properties. We observed expression of the photoreceptor-specific transcription factors (Crx—both rods and cones; Nr1—rods) and visual pigment rhodopsin together with structural protein ROM1. The differentiation pattern of hRPC was similar on PCL-IPM and fibronectin-coated scaffolds.

We suggest that the designed scaffold can be readily used as a bioreactor for the differentiation of photoreceptors and photoreceptor precursors, although its utility for transplantation has to be addressed in future studies, primarily due to the immunogenicity of IPM components, including interphotoreceptor retinoid-binding protein.<sup>41,42</sup>

## Conclusion

Here we have described an approach to functionalize PCL biopolymer with a water-insoluble IPM. This approach overcomes both the lack of cell adhesion, specific for hydrophobic PCL, and water insolubility of IPM, which complicates its use *in vitro*. We have shown that the resulting composite scaffolds drive the hRPC fate toward photoreceptors, allowing one to create a graft for subretinal transplantation and retinal regeneration, although the immune component of IPM transplantation should be addressed. We suggest that incorporation of ECM into PCL film may be a useful approach if composite sheet grafts are required, as it is in case of epithelium or neuroepithelium regeneration.

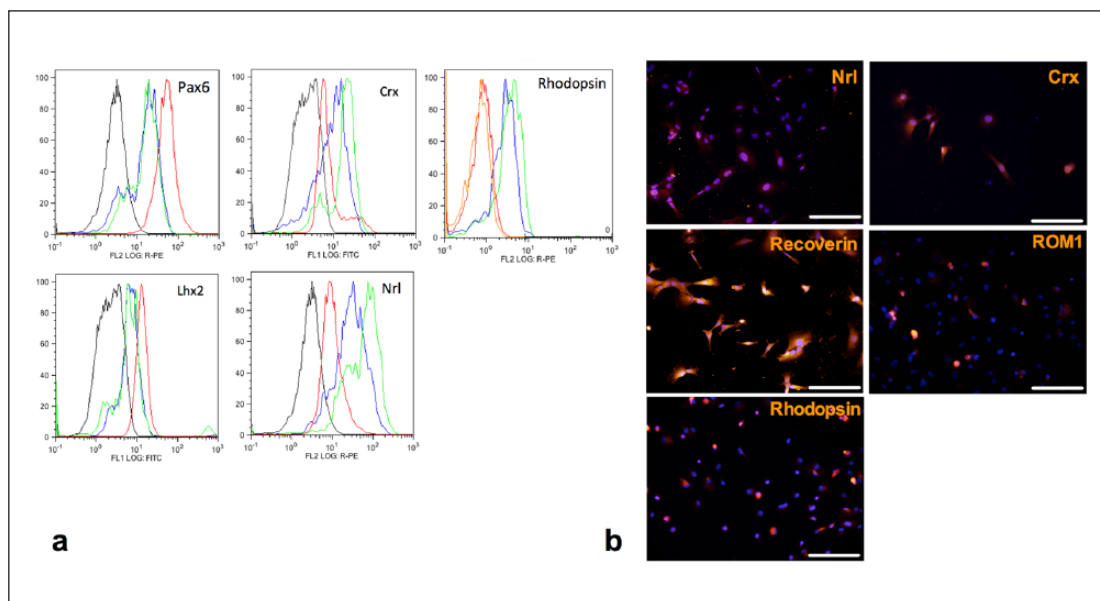


**Figure 4.** Differentiation of hRPC on PCL-IPM. (a) Flow cytometry analysis showed the downregulation of early eye development transcription factors Pax6 and Lhx2 in hRPC after 7 days of differentiation on both PCL coated with fibronectin (blue) and PCL-IPM (green) versus undifferentiated hRPCs (red). These results correlated with increase in photoreceptor-specific transcription factors (Crx and Nrl) and rod-specific rhodopsin and ROM1. Isotype controls are shown in black. (b) Immunocytochemical analysis of hRPC after differentiation confirmed the flow cytometry findings with individual cells expressing rhodopsin and ROM1 in polarized manner.

hRPC: human retinal progenitor cell; PCL: poly( $\epsilon$ -caprolactone); IPM: interphotoreceptor matrix.

## Acknowledgements

The authors thank William Fowle for his help with SEM sample preparation and imaging.

## Declaration of conflicting interests

The authors declare that there is no conflict of interest.

## Funding

This work was supported by NIH R21 1R21EY021312, ReNeuron Ltd (UK).

## References

1. Singh MS and MacLaren RE. Stem cells as a therapeutic tool for the blind: biology and future prospects. *Proc Biol Sci* 2011; 278(1721): 3009–3016.
2. MacLaren RE, Pearson RA, MacNeil A, et al. Retinal repair by transplantation of photoreceptor precursors. *Nature* 2006; 444(7116): 203–207.
3. Klassen H, Kiilgaard JF, Zahir T, et al. Progenitor cells from the porcine neural retina express photoreceptor markers after transplantation to the subretinal space of allorecipients. *Stem Cells* 2007; 25(5): 1222–1230.
4. Aftab U, Jiang C, Tucker B, et al. Growth kinetics and transplantation of human retinal progenitor cells. *Exp Eye Res* 2009; 89(3): 301–310.
5. Hynes SR and Lavik EB. A tissue-engineered approach towards retinal repair: scaffolds for cell transplantation to the subretinal space. *Graefes Arch Clin Exp Ophthalmol* 2010; 248(6): 763–778.
6. Zhang J, Skardal A and Prestwich GD. Engineered extracellular matrices with cleavable crosslinkers for cell expansion and easy cell recovery. *Biomaterials* 2008; 29(34): 4521–4531.
7. Chu XH, Shi XL, Feng ZQ, et al. Chitosan nanofiber scaffold enhances hepatocyte adhesion and function. *Biotechnol Lett* 2009; 31(3): 347–352.
8. Zhang HL, Wu JJ, Ren HM, et al. Therapeutic effect of microencapsulated porcine retinal pigmented epithelial cells transplantation on rat model of Parkinson's disease. *Neurosci Bull* 2007; 23(3): 137–144.
9. Tomita M, Lavik E, Klassen H, et al. Biodegradable polymer composite grafts promote the survival and differentiation of retinal progenitor cells. *Stem Cells* 2005; 23(10): 1579–1588.
10. Tao S, Young C, Redenti S, et al. Survival, migration and differentiation of retinal progenitor cells transplanted on micro-machined poly(methyl methacrylate) scaffolds to the subretinal space. *Lab Chip* 2007; 7(6): 695–701.
11. Sundback CA, Shyu JY, Wang Y, et al. Biocompatibility analysis of poly(glycerol sebacate) as a nerve guide material. *Biomaterials* 2005; 26(27): 5454–5464.
12. Kuo YC and Huang MJ. Material-driven differentiation of induced pluripotent stem cells in neuron growth factor-grafted poly( $\epsilon$ -caprolactone)-poly( $\beta$ -hydroxybutyrate) scaffolds. *Biomaterials* 2012; 33: 5672–5682.
13. Redenti S, Tao S, Yang J, et al. Retinal tissue engineering using mouse retinal progenitor cells and a novel biodegradable, thin-film poly( $\epsilon$ -caprolactone) nanowire scaffold. *J Ocul Biol Dis Infor* 2008; 1(1): 19–29.



14. Yao J, Tao SL and Young MJ. Synthetic polymer scaffolds for stem cell transplantation in retinal tissue engineering. *Polymers* 2011; 3(2): 899–914.
15. Nisbet DR, Yu LM, Zahir T, et al. Characterization of neural stem cells on electrospun poly(epsilon-caprolactone) submicron scaffolds: evaluating their potential in neural tissue engineering. *J Biomater Sci Polym Ed* 2008; 19(5): 623–634.
16. Lee Y-S and Livingston Arinze T. Electrospun nanofibrous materials for neural tissue engineering. *Polymers* 2011; 3(1): 413–426.
17. Fu X, Sammons RL, Bertóti I, et al. Active screen plasma surface modification of polycaprolactone to improve cell attachment. *J Biomed Mater Res B Appl Biomater* 2012; 100: 314–320.
18. Ghasemi-Mobarakeh L, Prabhakaran MP, Morshed M, et al. Bio-functionalized PCL nanofibrous scaffolds for nerve tissue engineering. *Mater Sci Eng C Mater Biol Appl* 2010; 30(8): 1129–1136.
19. Sadr N, Pippenger BE, Scherberich A, et al. Enhancing the biological performance of synthetic polymeric materials by decoration with engineered, decellularized extracellular matrix. *Biomaterials* 2012; 33(20): 5085–5093.
20. Tien L, Rayborn ME and Hollyfield JG. Characterization of the interphotoreceptor matrix surrounding rod photoreceptors in the human retina. *Exp Eye Res* 1992; 55(2): 297–306.
21. Hollyfield JG. Hyaluronan and the functional organization of the interphotoreceptor matrix. *Invest Ophthalmol Vis Sci* 1999; 40(12): 2767–2769.
22. Adler AJ and Edwards RB. Human interphotoreceptor matrix contains serum albumin and retinol-binding protein. *Exp Eye Res* 2000; 70(2): 227–234.
23. Klassen H, Ziacian B, Kirov II, et al. Isolation of retinal progenitor cells from post-mortem human tissue and comparison with autologous brain progenitors. *J Neurosci Res* 2004; 77(3): 334–343.
24. Baranov P, Regatieri C, Melo G, et al. Synthetic peptide-acrylate surface for self-renewal of human retinal progenitor cells. *Tissue Eng Part C Methods* 2013; 19(4): 265–270.
25. Osakada F, Hirami Y and Takahashi M. Stem cell biology and cell transplantation therapy in the retina. *Biotechnol Genet Eng Rev* 2010; 26: 297–334.
26. Pearson RA, Barber AC, Rizzi M, et al. Restoration of vision after transplantation of photoreceptors. *Nature* 2012; 485(7396): 99–103.
27. Gilbert TW, Sellaro TL and Badylak SF. Decellularization of tissues and organs. *Biomaterials* 2006; 27(19): 3675–3683.
28. Quint C, Kondo Y, Manson RJ, et al. Decellularized tissue-engineered blood vessel as an arterial conduit. *Proc Natl Acad Sci U S A* 2011; 108(22): 9214–9219.
29. Remlinger NT, Czajka CA, Juhas ME, et al. Hydrated xenogeneic decellularized tracheal matrix as a scaffold for tracheal reconstruction. *Biomaterials* 2010; 31(13): 3520–3526.
30. Ott HC, Matthiesen TS, Goh S-K, et al. Perfusion-decellularized matrix: using nature's platform to engineer a bioartificial heart. *Nat Med* 2008; 14(2): 213–221.
31. Price AP, England KA, Matson AM, et al. Development of a decellularized lung bioreactor system for bioengineering the lung: the matrix reloaded. *Tissue Eng Part A* 2010; 16(8): 2581–2591.
32. Uygun BE, Soto-Gutierrez A, Yagi H, et al. Organ reengineering through development of a transplantable recellularized liver graft using decellularized liver matrix. *Nat Med* 2010; 16(7): 814–820.
33. Zhou P, Lessa N, Estrada DC, et al. Decellularized liver matrix as a carrier for the transplantation of human fetal and primary hepatocytes in mice. *Liver Transpl* 2011; 17(4): 418–427.
34. Mieziwska K, Szél A, Van Veen T, et al. Redistribution of insoluble interphotoreceptor matrix components during photoreceptor differentiation in the mouse retina. *J Comp Neurol* 1994; 345(1): 115–124.
35. Hashimoto Y, Funamoto S, Kimura T, et al. The effect of decellularized bone/bone marrow produced by high-hydrostatic pressurization on the osteogenic differentiation of mesenchymal stem cells. *Biomaterials* 2011; 32(29): 7060–7067.
36. Traphagen SB, Fourligas N, Xylas JF, et al. Characterization of natural, decellularized and reseeded porcine tooth bud matrices. *Biomaterials* 2012; 33(21): 5287–5296.
37. Redenti S, Neeley WL, Rompani S, et al. Engineering retinal progenitor cell and scrollable poly(glycerol-sebacate) composites for expansion and subretinal transplantation. *Biomaterials* 2009; 30(20): 3405–3414.
38. Christiansen AT, Tao SL, Smith M, et al. Subretinal implantation of electrospun, short nanowire, and smooth poly(epsilon-caprolactone) scaffolds to the subretinal space of porcine eyes. *Stem Cells Int* 2012; 2012: 454295.
39. Regatieri CV, Baranov P, Carvalho A, et al. Pre differentiated human retinal progenitor cells integrate and express mature markers on the host retina. In: *ARVO2012*, Fort Lauderdale, FL, 6–9 May 2012, program/poster no. 1128/A593. Rockville, MD: ARVO.
40. Hageman GS and Johnson LV. Biochemical characterization of the major peanut-agglutinin-binding glycoproteins in vertebrate retinæ. *J Comp Neurol* 1986; 249(4): 499–510, 482–483.
41. Sanui H, Redmond TM, Hu L-H, et al. Synthetic peptides derived from IRBP induce EAU and EAP in Lewis rats. *Curr Eye Res* 2009; 7(7): 727–735.
42. Avichezer D, Silver PB, Chan CC, et al. Identification of a new epitope of human IRBP that induces autoimmune uveoretinitis in mice of the H-2b haplotype. *Invest Ophthalmol Vis Sci* 2000; 41(1): 127–131.